

LASER TECHNOLOGIES

PACS numbers: 81.15.Fg; 85.60.Ha; 85.60.Dw
DOI: 10.1070/QE2012v042n12ABEH014916

Fabrication of alkali halide UV photocathodes by pulsed laser deposition

V.M. Brendel, V.V. Bukin, S.V. Garnov, V.Kh. Bagdasarov, N.N. Denisov, S.G. Garanin, V.A. Terekhin, Yu.A. Trutnev

Abstract. **A technique has been proposed for the fabrication of atmospheric corrosion resistant alkali halide UV photocathodes by pulsed laser deposition. We produced photocathodes with a highly homogeneous photoemissive layer well-adherent to the substrate. The photocathodes were mounted in a vacuum photodiode, and a tungsten grid was used as an anode. Using pulsed UV lasers, we carried out experiments aimed at evaluating the quantum efficiency of the photocathodes. With a dc voltage applied between the photocathode and anode grid, we measured a shunt signal proportional to the total charge emitted by the cathode exposed to UV laser light. The proposed deposition technique enables one to produce photocathodes with photoemissive layers highly uniform in quantum efficiency, which is its main advantage over thin film growth by resistive evaporation.**

Keywords: *photocathode, PLD, photoemission, quantum yield.*

1. Introduction

UV photocathodes are being used increasingly, e.g. as UV detectors and electron injectors of particle accelerators. Of particular interest is the possibility to produce large-area photocathodes (more than 200 mm in diameter) possessing high quantum efficiency and a homogeneous photoemissive layer.

Pure metals have low quantum efficiency even after laser surface cleaning with the aim of removing impurities that increase their electronic work function [1]. The growth of a thin film of halide compounds on a metallic substrate is widely used to increase the quantum yield. The deposition process usually requires an expensive, high-vacuum equipment, complex target heating system or precision process control instrumentation. At the same time, even with such instrumentation the ability to grow e.g. caesium thin films requires considerable time for process optimisation.

Cultrera et al. [2] grew thin magnesium films from a laser-induced plasma generated by ablating a target with a high-power pulsed laser beam (pulsed laser deposition, PLD). The films thus produced offered good homogeneity and stoichiometry, high purity, strong adhesion and high quantum efficiency, comparable to that of films produced by conventional thermal evaporation of source material.

Thin halide films grown on metallic substrates are known to substantially improve the quantum efficiency of pure metals [3–6]. Such coatings are stable to harsh environments, which significantly simplifies the photocathode sealing process, especially at large electron-emitting surface areas.

In this work, halide (CsI and CsBr) films were grown by PLD, the quantum efficiency of the photocathodes thus produced was measured, and the homogeneity and adhesion of the PLD-grown photoemissive layers were compared to those of layers grown by thermal evaporation.

2. Photocathode fabrication by PLD

The PLD process has long been used to grow thin films and currently continues to develop. Pulsed laser deposition is particularly effective in producing coatings of complex stoichiometry. It offers a high film growth rate and is flexible and easy to control. Its drawbacks include the formation of large particles on the coating under improper laser operation conditions.

Pulsed laser deposition involves a variety of processes, which can be divided into three groups:

laser–target interaction (electromagnetic energy absorption, heating and melting of the target material and its vaporisation),

expansion of the plasma plume (initial plasma temperature in the plume, 5000–15000 K) and

deposition of the target material onto the substrate surface.

To produce halide coatings by PLD, we designed and fabricated a system that comprised the following units (Fig. 1): a vacuum chamber fitted with a target holder, substrate holder and a laser beam window; an Edwards WRG-S vacuum gauge; a piston pump backing a Varian S.p.A. turbomolecular pump; a lamp-pumped pulsed Nd:YAG laser with a LiF

V.M. Brendel, V.V. Bukin, S.V. Garnov, V.Kh. Bagdasarov, N.N. Denisov A.M. Prokhorov General Physics Institute, Russian Academy of Sciences, ul. Vavilova 38, 119991 Moscow, Russia; e-mail: vadim-boss@mail.ru, vladimir.bukin@gmail.com;
S.G. Garanin Institute of Laser Physics Research, Russian Federal Nuclear Center 'All-Russia Research Institute of Experimental Physics', prosp. Mira 37, 607188 Sarov, Nizhnii Novgorod region, Russia;
V.A. Terekhin Institute of Theoretical and Mathematical Physics, Russian Federal Nuclear Center 'All-Russia Research Institute of Experimental Physics', prosp. Mira 37, 607188 Sarov, Nizhnii Novgorod region, Russia;
Yu.A. Trutnev Russian Federal Nuclear Center 'All-Russia Research Institute of Experimental Physics', prosp. Mira 37, 607188 Sarov, Nizhnii Novgorod region, Russia

Received 14 June 2012; revision received 27 July 2012
Kvantovaya Elektronika **42** (12) 1128–1132 (2012)
Translated by O.M. Tsarev

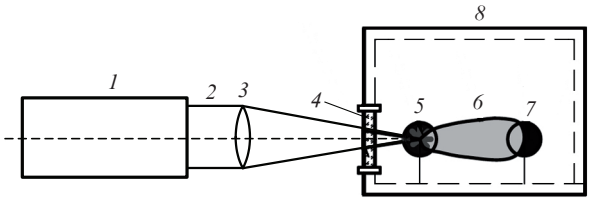

Figure 1. Schematic diagram of thin-film growth by pulsed laser deposition: (*1*) pulsed laser, (*2*) laser beam, (*3*) focusing optics, (*4*) quartz window, (*5*) target, (*6*) plasma plume, (*7*) substrate, (*8*) vacuum chamber.

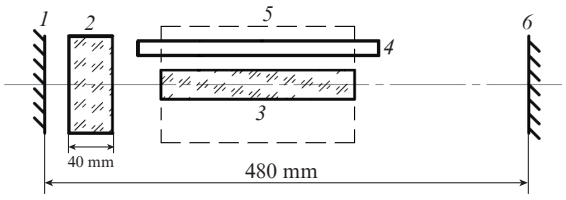

Figure 2. Pulsed Nd : YAG laser configuration: (*1*) high-reflectivity flat mirror, (*2*) LiF passive Q-switch ($T_0 = 5\%$), (*3*) gain element 6.3 mm in diameter and 100 mm in length (1.1% Nd), (*4*) pulsed xenon lamp, (*5*) elliptical reflector, (*6*) flat output coupler ($T = 40\%$).

saturable absorber; an $f = 50$ mm optical system that focused the laser beam onto the target; and a contactless heater that comprised a fibre-pigtailed semiconductor laser (808 nm, 9 W) and collimating objective.

The substrates used were copper and nickel plates 1.5 mm in thickness and 25 mm in diameter. The first step in thin-film growth is target and substrate preparation. If the source material for the coating is in powder form (CsBr in our case), it should be pressed into a pellet. The density of the pressed material should be high enough that, in the PLD process, the laser beam should not penetrate deep into the target (no deeper than 2–3 mm, i.e., the depth of focus of the laser beam), otherwise the deposition process is ineffective. If the material has the form of a single crystal (CsI) or another dense material, no target preparation steps are needed.

In designing the photocathode fabrication process, it became clear that a key condition for the ability to produce a homogeneous photoemissive coating possessing high quantum efficiency was quality substrate preparation, which involved several steps: mechanical cleaning, laser cleaning, chemical cleaning in a 50% hydrochloric acid solution, rinsing with distilled water and drying at room temperature. Deviations from this substrate cleaning procedure led to a significant drop in the quantum efficiency and homogeneity of the photocathode.

The substrate and target thus prepared were mounted parallel to one another in the vacuum chamber. The angle of incidence of the laser beam was varied from 45° to 90°, depending on the target density (the higher the target density, the smaller the angle). The vacuum chamber was pumped down to a residual pressure of 10^{-5} to 10^{-4} Torr, which was quite sufficient for producing a quality coating. The PLD process does not require high vacuum because the velocity of the particles in the plasma plume is as high as $\sim 10^4$ m s^{-1}, and the particles have no time to interact with impurities in the chamber. To improve coating adhesion to the substrate, it was heated to 60°C by the semiconductor laser beam, which penetrated the chamber through the quartz window. The substrate temperature was monitored with a thermocouple or noncontact thermometer.

After the substrate was heated to 60°C, a focused pulsed laser beam was directed to the target surface. We designed a lamp-pumped pulsed Nd : YAG laser with a LiF passive Q-switch (Fig. 2). The saturable absorber was mounted near the high-reflectivity mirror, and its position was adjusted so as to minimise the pulse duration. The laser generated single-mode 100-ns pulses at 1064 nm, with a pulse energy under 1 J and a pulse repetition rate no faster than 20 Hz.

The laser output power and pulse repetition rate were tuned in a wide range by controlling the power supply unit of the pulsed lamp. To obtain quality coating, the laser pulse power density should be only slightly higher than the laser plasma formation threshold, otherwise large particles are likely to be ejected from the target and deposited onto the substrate, degrading the quality of the coating. The deposition time (Fig. 3) was optimised experimentally and depended on the target material, its density and intended film thickness. At a laser pulse repetition rate of 20 Hz, the growth of thin films (several tens of nanometres in thickness) from dense target materials (CsI crystal and CsBr compact) took 1–2 min. The diffusion of particles from the plasma plume to the substrate material in the deposition process can be accelerated by heating the substrate. Quantum efficiency is known to reach its highest level at a film thickness of 0.5 μm [3]. Further increasing the film thickness causes no increase in quantum efficiency. In our experiments, we determined the deposition time corresponding to film thicknesses in the range 0.5–0.7 μm: ~16 min at a laser pulse repetition rate of 20 Hz. The thickness of the films was determined using an interferometer.

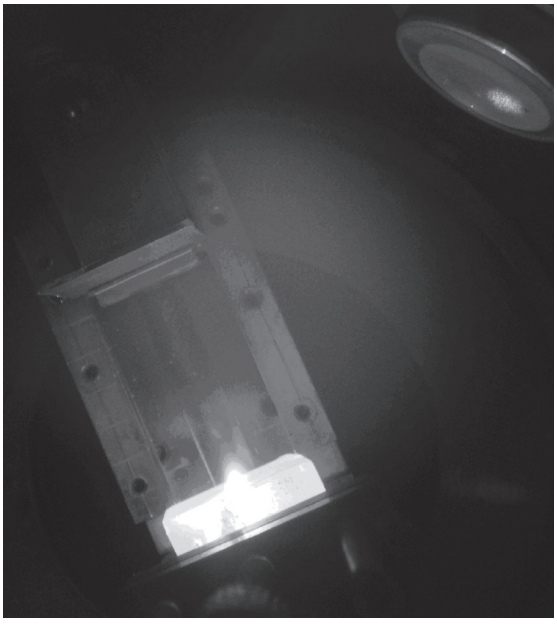

Figure 3. Photograph of the plasma plume used in CsI deposition onto a copper substrate.

After the laser deposition process, the substrate was left in the chamber and annealed at 60°C for 3 h. The anneal substantially improved the quantum yield of the photocathode because it eliminated undesirable impurities (for the most part, water vapour) from the film. Next, the sample was withdrawn from the vacuum chamber, held in air for 10 min and then transferred to a system for quantum efficiency measurements.

3. Photocathode quantum efficiency measurements

The quantum efficiency of photocathodes was evaluated by measuring the charge accumulated in a measuring capacitor due to the photoemission current produced by laser pulses with varied spectral and temporal parameters.

Figure 4 shows a schematic diagram of the photocathode quantum efficiency measurement circuit. The grid–cathode separation was 1–5 mm. The measurement channel was protected from high voltage in the case of grid–cathode gap breakdown by a protective measuring capacitor ($C_m \sim 10$ nF). The charge from the photocathode charged the cable (of capacitance C_c). The charge was then evaluated from the measured recharge current pulse through the measuring resistor (R_m). Since the cable capacitance, C_c, was far less than the protective measuring capacitance, C_m, the shape of the main current pulse through the input resistor of an oscilloscope was not distorted relative to that when C_m was short-circuited. A digital storage oscilloscope was used to measure voltage pulses with a characteristic time $\tau = R_m C_c \sim 100$ μs. The area under the voltage pulse profile divided by the input resistance of the oscilloscope was the area under the current pulse profile, i.e. the total charge (Q) that left the cathode as a result of photoemission:

$$Q = \int_{-\infty}^{+\infty} I(t)\,\mathrm{d}t = \int_{-\infty}^{+\infty} \frac{V(t)}{R_m}\,\mathrm{d}t, \tag{1}$$

where Q is the charge (in coulombs); $I(t)$ is the time-dependent current (in amperes); $V(t)$ is the time-dependent voltage (in volts); R_m is the resistance (in ohms); and t is time (in seconds).

From the charge Q thus determined and the measured laser pulse energy W (in electronvolts), we evaluated the quantum efficiency as

$$Y = \frac{N_{el}}{N_{ph}} = \frac{Q}{W}\frac{\hbar\omega}{e}, \tag{2}$$

where N_{el} and N_{ph} are the number of emitted photoelectrons and the number of photons incident on the cathode, respectively; $\hbar\omega$ is the photon energy (in electronvolts); and e is the elementary charge (in coulombs).

To determine the charge that passed through the measuring resistor when the photocathode was recharged, we evaluated the area under the current pulse profile without any assumptions as to the shape of the recharge current pulse. Owing to this, the stray inductances or capacitances present in the circuit had no effect on the charge thus found.

Note that there was no dc coupling between the cathode and measuring resistor owing to the protective capacitor. Because of this, the measuring capacitor was charged after a laser pulse. Before subsequent measurements, the charge was removed by closing the switch S.

To remove all of the charge, a rather high voltage had to be applied across the grid–cathode gap. The reason for this is that, when photoelectrons are emitted in a concentration exceeding the surface charge density of the grid–cathode capacitor, only part of the charge leaves the cathode. At a field strength $E = 1$ kV cm^{-1}, the surface charge density σ in the capacitor was 89 pC cm^{-2}. Since the energy density Φ of the laser sources used was within 1 mJ cm^{-2}, we had to reduce the laser beam intensity and increase the voltage applied across the grid–cathode gap in order to ensure removal of all the charge. For $\sigma\hbar\omega/e < Y\Phi$, the removed charge was an almost linear function of applied voltage. Note that, determining the saturation voltage starting at which there is no linear relation and the removed charge is independent of applied voltage, we can find the quantum efficiency as

$$Y = \frac{\sigma_{sat}}{\Phi}\frac{\hbar\omega}{e}, \tag{3}$$

where σ_{sat} is the saturation charge density.

Relation (3) is however only valid when the electron time of flight from the cathode to the grid far exceeds the laser pulse duration. When a picosecond laser source is used, this condition is fulfilled and the calculated quantum efficiency differs little from the measured one. When photoexcitation was provided by excimer lasers with a pulse duration of 5–7 ns, the calculated quantum efficiency was lower than the measured one.

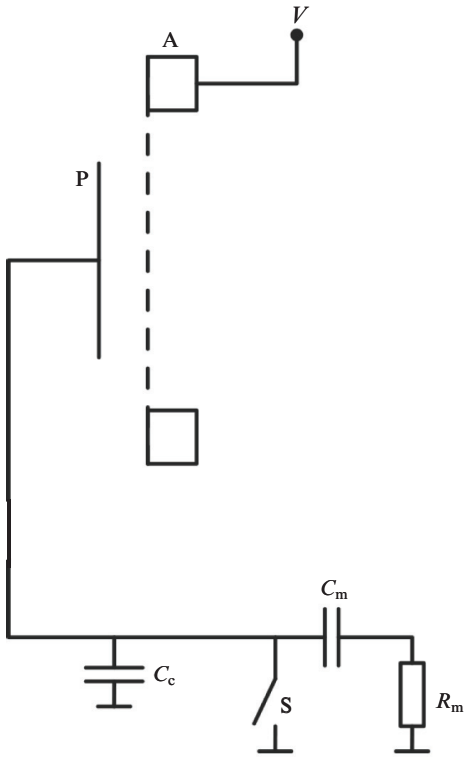

Figure 4. Schematic diagram of the photocathode quantum efficiency measurement circuit: (P) photocathode; (A) grid anode; (S) switch; (V) applied voltage, 0–20 kV; $C_c = 100$ pF; $C_m = 10$ nF; $R_m = 1$ MΩ.

A photocathode to be studied was mounted in a nonconductive Teflon holder (Fig. 5a). An anode was secured in the same holder 1 – 5 mm from the cathode (depending on the experiment). Basically, the assembly was a vacuum photodiode. The anode had the form of a grid with a transparency higher than 80%, made of 35-μm-diameter tungsten wire, which was strung with a pitch of 520 μm on a 50-mm-diameter copper ring. Figure 5b is a photograph of the grid.

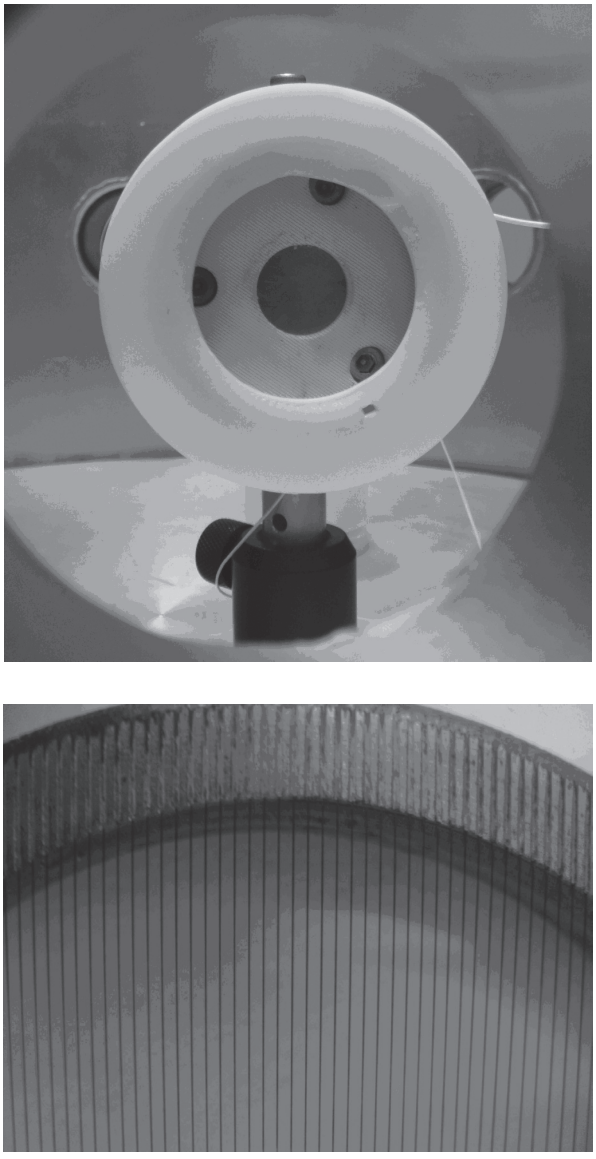

a

b

Figure 5. (a) Appearance of a photocathode, Teflon holder and grid in a vacuum chamber. (b) Photograph of the grid.

An SRS PS375 high-voltage power supply was used to apply a dc voltage less than 20 kV to the anode grid. The photocathode was connected to a Tektronix TDS 2022B or LeCroy WaveRunner 62Xi oscilloscope.

The cathode was exposed to laser pulses through the anode grid at normal incidence. The circuit under consideration allowed us to measure the total charge emitted by the photocathode during a laser pulse.

Measured quantum efficiency of CsI and CsBr photocathodes.

Photocathode material	Fabricatio technique	λ/nm	Y
CsI	PLD	193	1×10^{-2}
CsI	Resistive evaporation	193	1.5×10^{-2}
CsBr	PLD	193	3.3×10^{-3}
CsBr	PLD	248	1×10^{-4}

All quantum efficiency measurements were made in vacuum. To this end, the photocathode and anode grid, secured in the holder, were placed in a vacuum chamber fitted with quartz windows, which was then evacuated by a diaphragm pump (Adixen AMD4) and a turbomolecular pump (Adixen ATH200) to a residual pressure of 10^{-5} Torr. Cathode photoemission in the vacuum chamber was excited by a collimated (or focused by a CaF_2 lens) laser beam (spot diameter, 1 – 3 mm) introduced through the entrance quartz window. The laser pulse intensity on the photocathode surface was varied from 10^3 to 10^5 W cm^{-2}.

Electron emission was excited by ArF and KrF excimer lasers operating at 193 and 248 nm, respectively (pulse duration, 5 ns; repetition rate, 100 Hz). The quantum efficiencies obtained for different materials are presented in Table 1.

For comparison, a CsI photocathode was produced on a copper substrate by a conventional resistive evaporation process. The quantum efficiency of that photocathode approached that of the PLD photocathodes, but its photoemissive coating was significantly less homogeneous. When a laser beam was scanned over its surface, the quantum efficiency varied from zero to 100%. Beam scanning over the PLD photocathodes showed that the deviation from the highest efficiency level was within 20%. One of the PLD-grown photoemissive layer showed high wear resistance, indicating that it adhered well to the substrate.

4. Conclusions

Atmospheric corrosion resistant photocathodes have been produced by PLD. Our results demonstrate that careful substrate surface preparation is critical for the ability to produce a homogeneous photoemissive layer. The optimal angle of incidence of a laser beam ranges from 45° to 90° and decreases with increasing target density.

The quantum efficiencies obtained are lower than those reported previously [1]. The likely reason for this is that, when held in air for 10 min, a halide photoemissive coating absorbs an appreciable amount of water vapour, which considerably impairs its quantum efficiency. To increase it, the photocathode should be further annealed directly in the vacuum chamber. The PLD-grown photosensitive layers are shown to be more homogeneous and better adherent to the substrate than is a photocathode produced by resistive evaporation. Their quantum efficiency varies only slightly over the photocathode surface, which allows the PLD process to be applied in the fabrication of large-area UV photocathodes possessing high quantum efficiency throughout their photoemissive layer. Thus, pulsed laser deposition has considerable potential for producing high-performance UV photocathodes.

References

1. Buzulutskov A.F. *Fiz. Elem. Chastits At. Yadra*, **39** (3), 813 (2008).
2. Cultrera L. et al. *Phys. Rev. Spec. Top. Accel. Beams*, **12**, 043502 (2009).

3. Anderson D.F., Kwan S., Peskov V., Hoeneisen B. *Proc. Conf. on Advanced Technology and Particle Physics* (Como, Italy, 1992).
4. Maldonado J.R., Zhi Liu, Dowell D.H., Kirb R.E., Yun Sun, Pianetta P., Pease F. *Phys. Rev. Spec. Top. Accel. Beams*, **11**, 060702 (2008).
5. Charpak G., Lemenovski D., Peskov V., Scigocki D. *Nucl. Instum. Methods Phys. Res., Sect. A*, **310**, 128 (1991).
6. Buzulutskov A., Breskin A., Chechik R. *Nucl. Instum. Methods Phys. Res., Sect. A*, **366**, 410 (1995).